JOURNAL OF Materials CHEMISTRY

Aqueous acidic hydrogen peroxide as an efficient medium for tungsten insertion into MCM-41 mesoporous molecular sieves with high metal dispersion

Emmanuel Briot,[a] Jean-Yves Piquemal,[a] Maxence Vennat,[a] Jean-Marie Brégeault,*[a] Geneviève Chottard[b] and Jean-Marie Manoli[c]

[a]*Systèmes Interfaciaux à l'Echelle Nanométrique, Université Pierre et Marie Curie, CNRS-ESA 7069, Case 196, 4 place Jussieu, F-75252 Paris Cedex 05, France. E-mail: bregeaul@ccr.jussieu.fr*
[b]*Chimie Inorganique et Matériaux Moléculaires, Université Pierre et Marie Curie, CNRS-ESA 7071, Case 42, 4 place Jussieu, F-75252 Paris Cedex 05, France*
[c]*Réactivité de Surface, Université Pierre et Marie Curie, CNRS-UMR 7609, Case 178, 4 place Jussieu, F-75252 Paris Cedex 05, France*

Received 22nd October 1999, Accepted 26th January 2000

Two sets of WO_x/SiO_2-MCM-41 precatalysts (A and B) were prepared and compared. Tungsten-containing MCM-41 mesoporous molecular sieves have been synthesized with tetraethyl orthosilicate and tungsten precursors, tungstic acid, "H_2WO_4", or sodium tungstate, in the presence of cetyltrimethylammonium chloride (CTMACl) micelles as template in aqueous acid solution. In route A, H_2O_2 was added to avoid the formation of iso- (or hetero-) polyoxometalates in the counter-ion-mediated $S^+X^-I^+$ pathway with oxo–peroxo species [S^+ = quaternary ammonium ion surfactant, in this paper cetyltrimethylammonium ($CTMA^+$), $X^- = Cl^-$ and/or anionic peroxo species, I^+ = inorganic silicate precursor generating silanols or their protonated forms]. This procedure is compared with methods involving or generating polyoxometalates without peroxo moieties (route B) to determine whether the metal loading and/or dispersion is improved by H_2O_2. The native materials were calcined in air (1 K min^{-1}, isothermal at 920 K for 4 h) in order to decompose the organic template. The resulting molecular sieves have been characterized by chemical analysis, powder X-ray diffraction, UV-visible diffuse reflectance spectroscopy, nitrogen sorption isotherms, TEM and EDX analysis, and Raman spectrometry. High incorporation levels ($(Si:W)_{exp}$ molar ratio $\approx 30:1$) with a nearly homogeneous distribution of the dopants can be obtained only by route A. The spectral differences between the materials are correlated with their catalytic reactivities for cyclooctene epoxidation with an anhydrous H_2O_2/*t*-BuOH mixture at room temperature. The results suggest that the novel preparation method (route A) has a marked effect on the dispersion of the WO_x species on and into the silica matrix.

1 Introduction

Since the discovery of mesoporous materials M41S by the Mobil Research Laboratory in 1992,[1,2] several attempts have been made to incorporate transition metals such as Ti, V, Cr, Mn, W, Re, Zr, Mo into the hexagonal MCM-41 mesoporous structure. During the past five years great efforts[3–10] have been made to improve the tungsten dispersion onto silica,[3,5–7] alumina[4,6] or MCM-41.[6–10] The samples prepared from polyoxometalates contain crystalline tungsten oxide WO_3, whatever the preparation method.[3–5] Heteropolyacids, HPAs,[6–10] have been anchored onto these supports. In some cases, high HPA dispersion as well as high metal loading (up to 50 wt.% of HPA on siliceous MCM-41)[7] are obtained, but catalysis tests, when reported, show that only a small number of the redox and/or acid sites are active, which is confirmed by the low turnover numbers; water formed in some reaction tests can lead to formation of HPA clusters.[8] Moreover, only syntheses involving expensive organometallic precursors, such as [$W(\eta^3\text{-}C_3H_5)_4$], achieve highly dispersed surface tungsten oxide species.[3]

Several research groups have tried to synthesize mesoporous tungsten oxide materials or incorporate tungsten into mesoporous MCM-41 during synthesis. In 1994, Ciesla *et al.* were among the first to synthesize an all-tungsten oxide mesoporous MCM-41.[11] The as-synthesized material had the regular hexagonal array of uniform channels which is present in MCM-41, but calcination caused the mesostructure to collapse. Similar results were obtained by Stein *et al.*,[12] and they claimed that even the as-synthesized material consists mainly of unconnected Keggin ions $[H_2W_{12}O_{40}]^{6-}$. This result was confirmed with a different quaternary ammonium ion[13,14] or other Keggin anions.[14]

More recently, Zhang *et al.* described the synthesis of a tungsten-containing MCM-41.[15,16] They claimed that a $(Si:W)_{exp}$ molar ratio as low as 35 : 1 can be obtained using ammonium tungstate, "$(NH_4)_2WO_4$", as the source of tungsten, in order to achieve high metal dispersion. However, in the strongly acidic media used (addition of 5 mol dm^{-3} HCl), it may be inferred that oligomeric species are involved and give WO_3 upon calcination.[16] Indeed, it should be noted that monomeric species, *e.g.* $[WO_4]^{2-}$, are predominant at pH > 8 and low concentrations, but oligomeric non-peroxidic species, $[H_xW_yO_z]^{w-}$, are usually formed at high concentrations and low pH,[17–19] whereas several low-condensed neutral or anionic oxoperoxometalate species are generated at pH 1–2 in the presence of an excess of H_2O_2.[20,21] A problem remains: how to get a nearly homogeneous distribution of the dopant (WO_x species)?

In the present study two procedures are compared: (*i*) the oxo–peroxo mode "$H_2WO_4/H_2O_2/H_2O/H_3O^+$/templating agent/$Si(OEt)_4$", denoted route A, and (*ii*) the oxo–polyoxo

DOI: 10.1039/a908428b

synthesis "$Na_2WO_4{\cdot}2H_2O/H_2O/H_3O^+$/same template/$Si(OEt)_4$" (route B). The latter leads to iso- (or hetero-) polytungstates[17,18] such as $[H_2W_{12}O_{42}]^{10-}$, $[H_2W_{12}O_{40}]^{6-}$, while the former, with aqueous hydrogen peroxide, gives preferentially low-condensed oxo-peroxo species, *e.g.* $[WO(O_2)_2(H_2O)_2]$, $[O\{WO(O_2)_2\}_2]^{2-}$.[20–23] It is also known that $[SiO_4\{W_2O_2(\mu\text{-}O_2)_2(O_2)_2\}_2]^{4-}$, $[R_2SiO_2\{W_2O_2(\mu\text{-}O_2)_2(O_2)_2\}]^{2-}$, $[R_3SiO\{WO(O_2)_2\}]^-$, *etc.*[24,25] can be synthesized in the presence of silicic acid or silanols. These complexes are proposed as models for species such as neutral $\{W_2O_2(\mu\text{-}O_2)_2(O_2)_2\}$ and $\{WO(O_2)_2\}$ units grafted onto a silica surface *via* silanols.[25]

The oxo–peroxo route A leads to low-condensed species, which are more suitable than the HPAs for tungsten incorporation within the mesoporous silica framework, as was previously demonstrated with molybdenum.[26,27] All materials were characterized by chemical analysis, powder X-ray diffraction, TEM and EDX analysis, UV-visible diffuse reflectance spectroscopy, nitrogen adsorption–desorption and Raman spectrometry. Their activity in preliminary catalysis tests is also presented.

2 Experimental

2.1 Materials

Tetraethyl orthosilicate (TEOS) (purum 99%), cetyltrimethylammonium chloride (CTMACl) (25 wt.% in aqueous solution) and cyclooctene (95%) were purchased from Fluka. Tungstic acid, "H_2WO_4", was a gift from Eurotungsten. $Na_2WO_4{\cdot}2H_2O$ and 30 wt.% aqueous H_2O_2 (stabilizer: stannate) were commercial products (Prolabo). 37 wt.% HCl was purchased from Carlo Erba, *tert*-Butyl alcohol (>99%) from SDS. Ammonium metatungstate, $[NH_4]_6[\alpha\text{-}H_2W_{12}O_{40}]{\cdot}xH_2O$, and ammonium paratungstate B, $[NH_4]_{10}[H_2W_{12}O_{42}]{\cdot}4H_2O$, were prepared according to the literature.[17]

2.2 Syntheses

2.2.1 Route A. In a typical synthesis [$(Si:W)_{initial}$ (mol/mol) $\approx 40:1$], a counter-ion-mediated $S^+X^-I^+$ pathway was used in an acidic medium (S^+ = quaternary ammonium ion of surfactant, $X^-=Cl^-$ and/or peroxide, I^+ = inorganic silicate precursor). "H_2WO_4" (0.78 g; 3.1 mmol) was first treated with 30 wt.% aqueous hydrogen peroxide (2.5 mL; 24.5 mmol) to generate soluble low-condensed peroxo species (solution S1) after 1 h stirring at 60 °C, mainly $[WO(O_2)_2(H_2O)_2]$ and $[O\{WO(O_2)_2\}]^{2-}$.[21,22] The solution was then cooled at room temperature and centrifuged for 15 min at 2000 rpm to remove the unreacted "tungstic acid". TEOS (28 mL; 0.125 mol) was mixed with a solution containing the templating agent CTMACl (20 mL; 15 mmol) and HCl (12.5 M; 92 mL; 1.15 mol) in H_2O (218 mL; 12.1 mol), and solution S1 (W: 3.1 mmol) was added. The synthesis gel composition was: 1 TEOS/0.12 CTMACl/8.9 HCl/136 H_2O/0.19 H_2O_2/0.025 WO_3. The reaction mixture was stirred moderately (200 rpm) at room temperature for 2 h. The white precipitate was suction-filtered, washed with distilled water and dried over P_4O_{10} to give the native sample, denoted An. After drying overnight at room temperature, the white powder was calcined in air (200 $cm^3\ min^{-1}$; 1 K min^{-1}) from ambient to 920 K (samples maintained at the final temperature for 4 h) to remove the templating agent and give sample Ac.

2.2.2 Route B. Syntheses [$(Si:W)_{initial}$ (mol/mol) $\approx 40:1$] were adapted from methods previously described for molybdenum-containing MCM-41.[28] To a solution containing CTMACl (20 mL; 15 mmol) and HCl (12.5 M; 92 mL; 1.15 mol) in H_2O (222 mL; 12.3 mol) were added the transition metal ion precursor, $Na_2WO_4{\cdot}2H_2O$ (1.03 g; 3.1 mmol) and TEOS (28 mL; 0.125 mol). The synthesis gel composition was approximately: 1 TEOS/0.12 CTMACl/9.2 HCl/135 H_2O/0.025 WO_3. The reaction mixture was stirred vigorously at ambient temperature for 2 h. The pale yellow metallosilicate was then filtered off, washed with distilled water and air-dried over P_4O_{10} to give the native sample, Bn. The product was calcined as for sample An to remove the template, leading to sample Bc.

2.3 Apparatus

X-Ray diffraction patterns were recorded on a Siemens D500 diffractometer (Cu-Kα radiation) with 0.02° (2θ) step size and 8 s step time generally in the range $1.7<2\theta<15°$. Adsorption and desorption isotherms for nitrogen were obtained at 77 K using a Micromeritics ASAP 2010. The samples were outgassed at 393 K and 0.1 Pa for 12 h before measurements. Specific surface area values were obtained using the BET (Brunauer–Emmett–Teller) equation; the mean pore sizes are those of the BJH (Barrett–Joyner–Halenda) method, with the desorption branch being analysed.[29,30] UV-visible diffuse reflectance spectroscopy was performed on a Varian Cary 5E spectrophotometer equipped with an integration sphere and coupled to a computer. Polytetrafluoroethylene was used as reference. Transmission Electron Microscopy (TEM) and Energy Dispersive X-ray Analysis (EDX) were performed using a Link AN 10000 system (Si–Li diode detector) connected to a JEOL JEM 100 CXII transmission electron microscope operating at 100 kV and equipped with an ASID 4D scanning device (STEM mode). The X-rays emitted from the specimen upon electron impact from rectangular domains (*e.g.* $150\times200\ nm^2$) were collected in the 0–20 keV range for 400 s with [$Si_{K\alpha}+W_M$] and W_L lines. Since the instrument is not sensitive to oxygen the data do not include the oxygen content. Elemental analyses were carried out at the Service Central d'Analyse (CNRS-Lyon) by inductively coupled plasma atomic emission spectroscopy (ICP-AES) after alkaline fusion with $Li_2B_4O_7$. The Raman spectra of the mesoporous solids were recorded at room temperature with a Jobin Yvon U1000 spectrometer (excitation line, 514.5 nm of an Ar^+ ion laser; source power, 30–50 mW; resolution, 4 cm^{-1}). Dehydrated samples are mounted on a rotating disk to avoid their decomposition and/or photoreduction by the laser beam.

2.4 Catalysis tests

Dry H_2O_2 was prepared by mixing 100 mL of *t*-BuOH, 30 mL of aqueous H_2O_2 30 wt.% and an excess of anhydrous $MgSO_4$ (*ca.* 15 g). In a typical test, with strirring at room temperature, 130 mg of catalyst were placed in a Schlenk tube with 8 mL of the H_2O_2/*t*-BuOH mixture (18 mmol H_2O_2) and 0.5 mL of cyclooctene (3.65 mmol). The progress of the reaction was monitored by GC (Delsi 30 gas chromatograph equipped with a 0.25 mm × 50 m OV1701 capillary column and a flame ionization detector linked to a Delsi Enica 10 electronic integrator). The products were analysed after quenching with MnO_2.

3 Results and discussion

3.1 Elemental analysis and X-ray diffraction

The X-ray diffraction patterns (Fig. 1) show the characteristic diagram of hexagonal mesoporous MCM-41. The low angle (2θ) large peak seen in the diagrams for the native and calcined samples can be indexed as (100), and other weak diffraction peaks, (110), (200), *etc.* indicate that the nearly amorphous materials are characterized by a short-range order. Based on hexagonal symmetry, the unit cell parameter a_0 can be calculated using the formula: $a_0=2d_{100}/\sqrt{3}$. Removal of the templating agent leads to a decrease in a_0 (*ca.* 8 Å), indicating

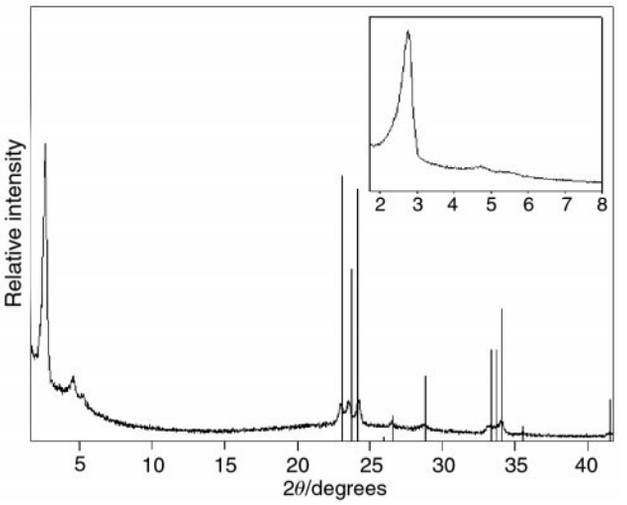

Fig. 1 X-Ray diffraction patterns of samples Bc and A1c (insert). Peaks relative to WO_3 (JCPDS 20-1324) are indicated on the diagram.

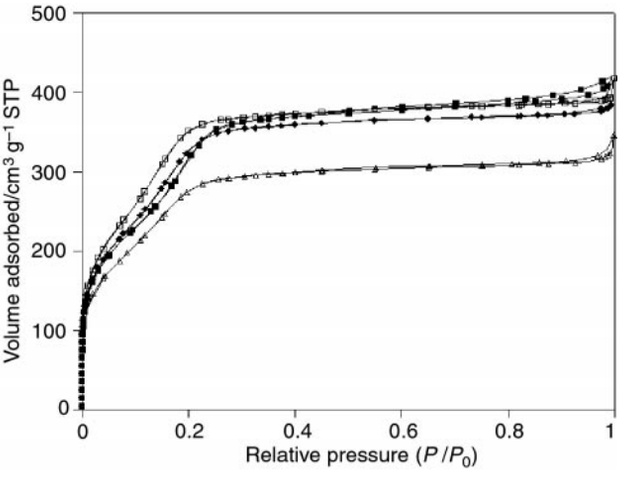

Fig. 2 Nitrogen sorption isotherms obtained at 77 K for samples all Si (□), A1c (◆), A2c (△) and Bc (■) (see Table 1). Adsorption and desorption branches are nearly coincident.

that the template acts as a directing agent and as a structure support (see Table 1).

All samples have similar X-ray patterns, except for Bc which displays three peaks at about $2\theta = 23^\circ$ attributed to crystalline WO_3 (Fig. 1); therefore, it should be noted that under our conditions route B (in a highly acidic medium) leads to phase segregation.

The experimental (Si : W) molar ratio matches the initial composition in the gel, which indicates that the amount of tungsten incorporated into MCM-41 can easily be adjusted whatever the $S^+X^-I^+$-mediated route (A or B) followed (Table 1).

3.2 Nitrogen sorption at 77 K

All samples exhibit a reversible, nearly hysteresis-free, type IV isotherm according to IUPAC nomenclature[29] (Fig. 2). The BET surface areas and the mean pore diameters, $Ø_{BJH}$, estimated by the BJH method are in the same range as that for purely siliceous MCM-41, as shown in Table 1; these results compare well with previous data for Mo-MCM-41.[27] Although it is well known that the BJH method underestimates the mean pore diameter,[31] values are in fair agreement with transmission electron microscopy measurements. The isotherm of sample A2c, prepared according to route A with a high initial concentration of the tungsten species, $(Si:W)_{initial} = 20:1$, is below the others. This could be explained by (*i*) phase segregation and/or by (*ii*) some degree of pore blocking with HPAs and/or polymeric species causing the surface area and pore volume to fall. With sample Bc ($(Si:W)_{initial} = 40:1$), oligomeric species are also formed (*vide infra* 3.4.–3.5), but they do not cause noticeable pore blocking.

3.3 Electron microscopy and EDX analysis

One representative TEM micrograph of sample A1c is shown in Fig. 3. Typical MCM-41 images with holes, representing the pore aperture, and channels confirm the mesoporous nature of the materials.

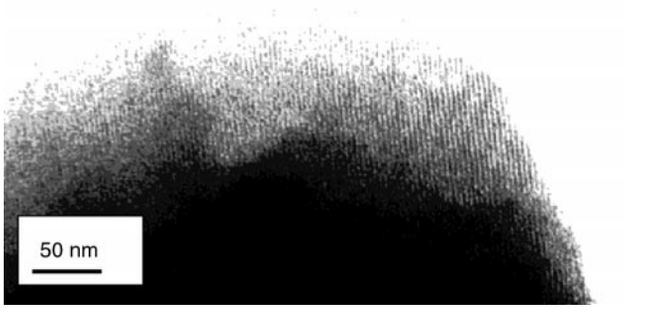

Fig. 3 Typical TEM micrograph of sample A1c.

With EDX analysis, a promising method for characterizing titanium silicalite[32] or MoO_x/siliceous MCM-41,[27] it appears difficult to quantify silicon and tungsten precisely, since the W_M emission line is located at nearly the same energy as that of the $Si_{K\alpha}$ emission line (*ca.* 1.74 keV). However, semi-quantitative information can be deduced from the $[Si + W_M] : [W_L]$ ratio. Indeed, a nearly homogeneous distribution of the dopant is observed in sample A1c. On the other hand, in sample A2c the $[Si + W_M] : [W_L]$ molar ratio depends markedly on the domain observed. This result confirms that phase segregation has occurred during the synthesis of sample A2c, leading to an inhomogeneous distribution of the tungsten species, with clusters on the outer surface. In sample Bc two or more phases are present as a consequence of phase segregation (*vide supra* 3.1 and *infra* 3.5).

3.4 UV-visible diffuse reflectance spectroscopy

The spectra of thermally treated products (Fig. 4) usually display broader bands than those obtained with native samples (not shown) and consist of high-energy maxima and broad

Table 1 Tungsten content, (Si/W) molar ratio, unit cell parameters, specific surface area, mean pore diameter ($Ø_{BJH}$) and wall thickness (w)

Run	Route	$(Si:W)_{initial}$	Si (wt.%)	W (wt.%)	$(Si:W)_{exp}$	$a_0{}^a$/Å	S_{BET}/m^2 g^{-1}	$Ø_{BJH}$/Å	w^b/Å
All Si	/	∞	/	/	∞	45.5 (36)	1384 ± 45	16	19.5
A1	oxo–peroxo	40	39.4	8.2	31	46 (37)	1253 ± 45	17	19.0
A2	oxo–peroxo	20	36.2	12.5	19	47 (37)	1067 ± 30	17	20.0
B	oxo–polyoxo	40	40.1	8.3	32	45 (38)	1203 ± 40	17	18.0

[a]Native samples. Numbers in parentheses represent the unit cell parameters of the calcined samples.[b]$w = a_0 - Ø_{BJH}$.

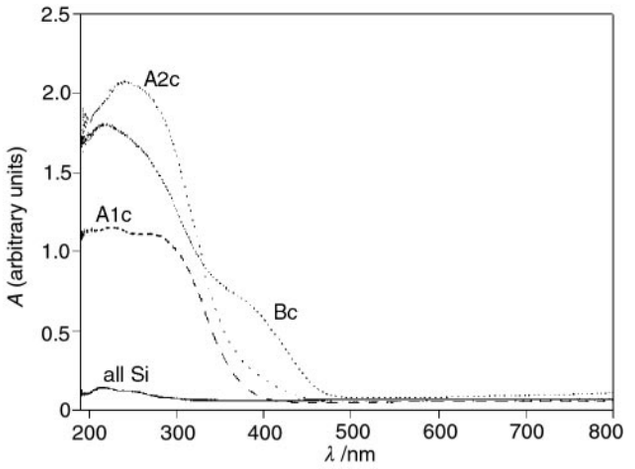

Fig. 4 UV-visible diffuse reflectance spectra of samples all Si, A1c, A2c and Bc.

absorption bands with superimposed shoulders. Fig. 5 shows clearly the differences between four standards. For sodium tungstate ($Na_2WO_4{\cdot}2H_2O$), with a spinel structure[33] and isolated $[WO_4]^{2-}$ tetrahedra, the spectrum is characterized by a maximum at 230 nm (*ca.* 5.4 eV). Ammonium metatungstate ($[NH_4]_6[\alpha\text{-}H_2W_{12}O_{40}]{\cdot}xH_2O$) and paratungstate ($[NH_4]_{10}[H_2W_{12}O_{42}]{\cdot}4H_2O$) present characteristic spectra with at least two maxima at 260 and 340 nm and at 230 and 320 nm, respectively (*ca.* 5 and 3.9 eV), and a shift towards higher wavelengths. These values are related to the oligomeric structure of these anions. The recent work of Weber[34] and Iglesia *et al.*[35] demonstrates that the low-energy absorption edge is shifted towards higher wavelengths when the nuclearity of molybdenum or tungsten entities increases, and is sensitive to domain size within the 1–10 nm range for many compounds including WO_3 (Fig. 5).

In the present study, the UV-visible absorption edge is clearly shifted towards higher wavelengths for samples A2c and Bc (Fig. 4), indicating the presence of oligomeric species, probably WO_3, in these samples, particularly for sample Bc; on the contrary, the spectrum of A1c may reflect the very high dispersion of the WO_x species; this will be confirmed by the Raman data.

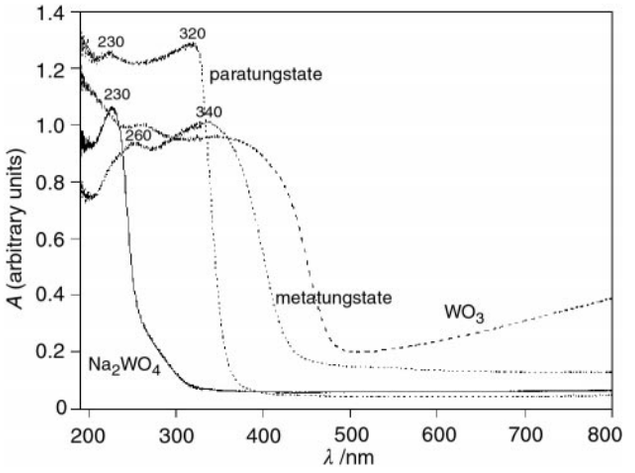

Fig. 5 UV-visible diffuse reflectance spectra of samples $Na_2WO_4{\cdot}2H_2O$, ammonium metatungstate $[NH_4]_6[\alpha\text{-}H_2W_{12}O_{40}]{\cdot}xH_2O$, ammonium paratungstate B $[NH_4]_{10}[H_2W_{12}O_{42}]{\cdot}4H_2O$ and WO_3.

3.5 Raman spectrometry

This method is very useful for the characterization of detemplated materials. The Raman spectra of the W-MCM-41 prepared by the oxo–peroxo route (A1c and A2c) and the oxo–polyoxo route (Bc) are shown in Fig. 6 with two reference spectra (high-purity mesoporous silica and crystalline WO_3). They include bands that originate from the SiO_2 matrix [*ca.* 1100 (very weak), 810, 613 and 493–500 cm^{-1}] as well as from the tungsten oxo species. Bands attributed to the symmetric stretching mode of the terminal W=O bonds are observed at 966, 964 and 969 cm^{-1}. This assignment is still questionable;[32] terminal Si–O stretching of SiOH···OW "defective sites" may also contribute.

For sample A1c (Fig. 6a) no Raman bands due to crystalline WO_3 (*vide infra*) or to "$WO_3{\cdot}2H_2O$"[36] [960 (sharp), 685–662 (broad), 380 and 268 cm^{-1}] are observed. On the contrary, the Raman spectrum of Bc materials (Fig. 6c), prepared by the aqueous method using $Na_2WO_4{\cdot}2H_2O$, exhibits strong bands due to crystalline WO_3[3,36,37] at 805, 711 and 272 cm^{-1}, which are assigned to the symmetric stretching modes and to the deformation mode (δ) of the O–W–O moieties. The observation of these very strong Raman features indicates the formation of a very poorly dispersed SiO_2-supported tungsten oxide phase. Therefore, when the sample is heated at elevated temperatures ($\approx$650 °C), the polytungstate ions transform readily into bulk WO_3 surface species.

The Raman spectrum of sample A2c (Fig. 6b) shows contributions from two materials: A1c and Bc. Indeed, bands attributed to W=O terminal groups and tungsten oxide are present; such typical curves for $(Si:W)_{exp} \leqslant 20:1$ show that the oxo–peroxo route does not give well dispersed W-containing MCM-41 materials. These results show that it is possible to achieve highly dispersed WO_x species in WO_x/

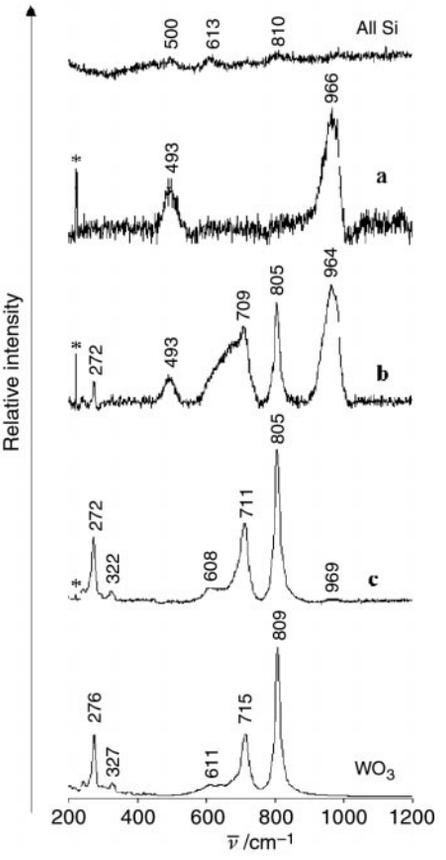

Fig. 6 Raman spectra of samples A1c (a), A2c (b), Bc (c), of high-purity mesoporous silica all Si and of tungsten trioxide WO_3. (*): plasma line.

Table 2 Cyclooctene epoxidation over various catalysts, after 24 hours reaction. In all cases there is 100% selectivity to epoxide[a]

Run	H_2O_2 : Substrate (mol/mol)	Substrate : W (mol/mol)	Cyclooctene conversion (%)
All Si	5	∞	0
A1c	5	63	98
A2c	5	42	84
Bc	5	62	33

[a]Reaction conditions: see text. Room temperature experiments.

siliceous MCM-41 precatalysts by a very simple aqueous method thus avoiding the need for an expensive precursor such as $[W(\eta^3\text{-}C_3H_5)_4]$ in a non-aqueous medium.[3]

3.6 Catalysis tests

The results of cyclooctene epoxidation over W-containing MCM-41 are listed in Table 2. Blank experiments with purely siliceous MCM-41 show that it is virtually inactive for this reaction at room temperature. In contrast, W-containing MCM-41 catalysts are very active, even at room temperature. Comparison of A1c and Bc indicates that materials synthesized by route A are distinctly more active. This can be explained by the presence of less active WO_3 material in the Bc sample. More interesting is the result obtained with sample A2c. Despite the high tungsten loading in A2c ($(Si:W)_{exp} = 20:1$) and the large amount of tungsten used during the catalysis test ($(Substrate:W) = 42:1$), cyclooctene conversion is less than that observed with A1c. This result can be understood by considering that sample A2c does not only contain isolated W species, but also tungsten oxide and/or HPA species which are poorer precatalysts for this reaction. Catalysis results match those obtained by different physicochemical techniques, especially Raman spectroscopy. Furthermore, atomic emission spectroscopic analysis of the epoxidation solutions indicates that there is reduced leaching (quantitative analysis is in progress) of W into the solutions. Work is in progress to obtain materials resistant to nucleophilic attack and to run tests with weak nucleophiles.

4 Conclusion

W-containing MCM-41 materials synthesized by the oxo–peroxo method (A) are obviously very promising catalysts not only in this environmentally and economically attractive oxidation but also in other reactions under study, such as metathesis. This activity can partially be explained by the high loading of the tungsten species with a nearly homogeneous distribution of the dopants. On the contrary, samples prepared according to the oxo–polyoxo route (B) or the oxo–peroxo (A) route with $(Si:W)_{exp}$ as low as 20 : 1 behave differently, probably due to the presence of WO_3 and/or HPA species. We think that the Chinese group worked with oxo-polyoxo species: pure ammonium tungstate cannot be the precursor involved in the synthesis; in reality, they worked with $[NH_4]_{10}[H_2W_{12}O_{42}]\cdot 4H_2O$, imprecisely denoted "ammonium tungstate", which give WO_3 upon calcination. Despite the marked improvement offered by the aqueous oxo–peroxo method, the chemical and mechanical stabilities of samples A need to be improved to avoid the leaching of redox-active species into the solution. New syntheses are being studied to develop mesoporous Mo- and W-containing MCM-41 with low leaching during liquid-phase reaction catalysis, since environmental and economic concerns may ultimately favour supported heterogeneous or genuinely two- or three-phase catalytic systems.

The very dispersive structure of the WO_x/siliceous MCM-41 promotes the generation of highly active catalysts. Our information remains limited on the mechanism of these reactions and on which factors, besides the fact that they have tungsten peroxo species for epoxidation, or surface carbene species for metathesis, influence the efficiency of these materials. Work is in progress to control these systems better and to optimize epoxidation and metathesis results.

Acknowledgements

We thank Dr. John Lomas for constructive discussions and for correcting the manuscript, and Professor Dr. F. Bozon-Verduraz for UV-visible spectroscopy facilities.

References

1 C. T. Kresge, M. E. Leonowicz, W. J. Roth, J. C. Vartuli and J. S. Beck, *Nature* (*London*), 1992, **359**, 710.
2 J. S. Beck, J. C. Vartuli, W. J. Roth, M. E. Leonowicz, C. T. Kresge, K. D. Schmitt, C. T. W. Chu, E. W. Sheppard, S. B. McCullen, J. B. Higgins and J. L. Schlenker, *J. Am. Chem. Soc.*, 1992, **114**, 10834.
3 D. S. Kim, M. Ostromecki, I. E. Wachs, S. D. Kohler and J. D. Ekerdt, *Catal. Lett.*, 1995, **33**, 209.
4 M. M. Ostromecki, L. J. Burcham, I. E. Wachs, N. Ramani and J. G. Ekerdt, *J. Mol. Catal. A: Chem.*, 1998, **132**, 43.
5 D. Juwiler, J. Blum and R. Neumann, *Chem. Commun.*, 1998, 1123.
6 C. T. Kresge, D. O. Marler, G. S. Rav and B. H. Rose, *U.S. Pat.*, 5,366,945, 1994.
7 I. V. Kozhevnikov, A. Sinnema, R. J. J. Jansen, K. Pamin and H. van Bekkum, *Catal. Lett.*, 1995, **30**, 241.
8 M. J. Verhoef, P. J. Kooyman, J. A. Peters and H. van Bekkum, *Microporous Mesoporous Mater.*, 1999, **27**, 365.
9 F. Marme, G. Coudurier and J. C. Védrine, *Microporous Mesoporous Mater.*, 1998, **22**, 151.
10 W. Chu, X. Yang, Y. Shan, X. Ye and Y. Wu, *Catal. Lett.*, 1996, **42**, 201.
11 U. Ciesla, D. Demuth, R. Leon, P. Petroff, G. Stucky, K. Unger and F. Schüth, *J. Chem. Soc., Chem. Commun.*, 1994, 1387.
12 A. Stein, M. Fendorf, T. P. Jarvie, K. T. Mueller, A. J. Benesi and T. E. Mallouk, *Chem. Mater.*, 1995, **7**, 304.
13 G. G. Janauer, A. Dobley, J. Guo, P. Zavalij and M. S. Whittingham, *Chem. Mater.*, 1996, **8**, 2096.
14 A. Tagushi, T. Abe and M. Iwamoto, *Microporous Mesoporous Mater.*, 1998, **21**, 387.
15 Z. Zhang, J. Suo, X. Zhang and S. Li, *Chem. Commun.*, 1998, 241.
16 Z. Zhang, J. Suo, X. Zhang and S. Li, *Appl. Catal., A: General*, 1999, **179**, 11.
17 M. T. Pope, *Heteropoly- and Isopolyoxometalates*, Springer-Verlag, Berlin, 1983.
18 J.-P. Jolivet, *De la Solution à l'Oxyde*, InterEditions/CNRS, Paris, 1994.
19 L. Karakonstantis, C. Kordulis and A. Lycourghiotis, *Langmuir*, 1992, **8**, 1318.
20 L. Salles, C. Aubry, R. Thouvenot, F. Robert, C. Dorémieux-Morin, G. Chottard, H. Ledon, Y. Jeannin and J.-M. Brégeault, *Inorg. Chem.*, 1994, **33**, 871.
21 J.-M. Brégeault, R. Thouvenot, S. Zoughebi, L. Salles, A. Atlamsami, E. Duprey, C. Aubry, F. Robert and G. Chottard, in *Studies in Surface Science and Catalysis, New Developments in Selective Oxidation II*, eds. V. Cortès Corberán and S. Vic Bellón, Elsevier, Amsterdam, 1994, vol. 82, p. 571.
22 H. Mimoun, in *The Chemistry of Functional Groups, Peroxides*, eds. S. Pataï, Wiley, New York, 1983, ch. 15.
23 M.-H. Dickman and M. T. Pope, *Chem. Rev.*, 1994, **94**, 625.
24 J.-Y. Piquemal, C. Bois and J.-M. Brégeault, *Chem. Commun.*, 1997, 473.
25 J.-Y. Piquemal, S. Halut and J.-M. Brégeault, *Angew. Chem., Int. Ed.*, 1998, **37**, 1146.

26 J.-Y. Piquemal, E. Briot, M. Vennat, J.-M. Brégeault, G. Chottard and J.-M. Manoli, *Chem. Commun.*, 1999, 1195.
27 J.-Y. Piquemal, J.-M. Manoli, P. Beaunier, A. Ensuque, P. Tougne, A.-P. Legrand and J.-M. Brégeault, *Microporous Mesoporous Mater.*, 1999, **29**, 291.
28 W. Zhang, J. Wang, P. T. Tanev and T. J. Pinnavaïa, *Chem. Commun.*, 1996, 979.
29 K. S. W. Sing, D. H. Everett, R. A. Haul, L. Moscou, R. A. Pierotti, J. Rouquérol and T. Siemieniewska, *Pure Appl. Chem.*, 1985, **57**, 603.
30 E. P. Barrett, L. G. Joyner and P. P. Halenda, *J. Am. Chem. Soc.*, 1951, **73**, 376.
31 M. Kruk, M. Jaroniec and A. Sayari, *Microporous Mater.*, 1997, **9**, 173.
32 E. Duprey, P. Beaunier, M.-A. Springuel-Huet, F. Bozon-Verduraz, J. Fraissard, J.-M. Manoli and J.-M. Brégeault, *J. Catal.*, 1997, **165**, 22.
33 C. W. F. T. Pistorius, *J. Chem. Phys.*, 1966, **44**, 4532.
34 R. S. Weber, *J. Catal.*, 1995, **151**, 470.
35 E. Iglesia, D. G. Barton, S. L. Soled, S. Miseo, J. E. Baumgartner, W. E. Gates, G. A. Fuentes and G. D. Meitzner, *Stud. Surf. Sci. Catal.*, 1996, **101**, 533.
36 M.-F. Daniel, B. Desbat, J.-C. Lassegues, B. Gerand and M. Figlarz, *J. Solid State Chem.*, 1987, **67**, 235.
37 S. Colque, E. Payen and P. Grange, *J. Mater. Chem.*, 1994, **4**, 1343.

Paper a908428b